Probiotic cellulose: Antibiotic-free Biomaterials with Enhanced Antibacterial Activity

Article *in* Acta Biomaterialia · January 2021

DOI: 10.1016/j.actbio.2021.01.039

CITATIONS
23

READS
597

9 authors, including:

Laura Sabio
University of Glasgow
10 PUBLICATIONS **186** CITATIONS
SEE PROFILE

Ana González
University of Granada
20 PUBLICATIONS **299** CITATIONS
SEE PROFILE

Gloria Belén Ramírez Rodríguez
University of Granada
55 PUBLICATIONS **1,038** CITATIONS
SEE PROFILE

José Gutiérrez-Fernández
University of Granada
470 PUBLICATIONS **3,902** CITATIONS
SEE PROFILE

Acta Biomaterialia xxx (xxxx) xxx

Contents lists available at ScienceDirect

Acta Biomaterialia

journal homepage: www.elsevier.com/locate/actbio

Probiotic cellulose: Antibiotic-free biomaterials with enhanced antibacterial activity

Laura Sabio[a], Ana González[a], Gloria B. Ramírez-Rodríguez[a], José Gutiérrez-Fernández[b], Oscar Bañuelo[c], Mónica Olivares[c], Natividad Gálvez[a], José M. Delgado-López[a,*], Jose M. Dominguez-Vera[a,*]

[a] Departamento de Química Inorgánica, Universidad de Granada, 18071 Granada, Spain
[b] Department of Microbiology, Virgen de las Nieves University Hospital, Granada, Spain
[c] Biosearch S. A. Camino de Purchil, 66, 18004 Granada, Spain

ARTICLE INFO

Article history:
Received 2 September 2020
Revised 25 January 2021
Accepted 26 January 2021
Available online xxx

Keywords:
Antibiotic-free biomaterials
Bacterial cellulose
Probiotic
Chronic wounds

ABSTRACT

The alarming increase of antibiotic-resistant bacteria, causing conventional treatments of bacterial infections to become increasingly inefficient, is one of the biggest threats to global health. Here, we have developed probiotic cellulose, an antibiotic-free biomaterial for the treatment of severe skin infections and chronic wounds. This composite biomaterial was in-depth characterized by Gram stain, scanning electron microscopy (SEM) and confocal fluorescence microscopy. Results demonstrated that probiotic cellulose consists of dense films of cellulose nanofibers, free of cellulose-producing bacteria, completely invaded by live probiotics (*Lactobacillus fermentum* or *Lactobacillus gasseri*). Viability assays, including time evolution of pH and reducing capacity against electrochromic polyoxometalate, confirmed that probiotics within the cellulose matrix are not only alive but also metabolically active, a key point for the use of probiotic cellulose as an antibiotic-free antibacterial biomaterial. Antibacterial assays in pathogen-favorable media, a real-life infection scenario, demonstrated that probiotic cellulose strongly reduces the viability of *Staphylococcus aureus (SA)* and *Pseudomonas aeruginosa (PA)*, the most active pathogens in severe skin infections and chronic wounds. Likewise, probiotic cellulose was also found to be effective to inhibit the proliferation of methicillin-resistant *SA (MRSA)*. The combination of the properties of bacterial cellulose as wound dressing biomaterial and the antibacterial activity of probiotics makes probiotic cellulose an alternative to antibiotics for the treatment of topical infections, including severe and hard-to-heal chronic wounds. In addition, probiotic cellulose was obtained by a one-pot synthetic approach under mild conditions, not requiring the long and expensive chemical treatments to purify the genuine bacterial cellulose.

Statement of significance

Antibiotic resistance is responsible for around 700.000 deaths per year worldwide, with the potential to cause 10 million deaths by 2050. New antibiotic-free approaches are thus urgently needed for the treatment and prevention of bacterial infections. We produced probiotic cellulose, which consists of dense films of cellulose nanofibers completely invaded by live and metabolically active probiotics. This antibiotic-free biomaterial exhibits excellent anti-bacterial activity against *Staphylococcus aureus* and *Pseudomonas aeruginosa*, the most active pathogens in skin infections and chronic wounds. Likewise, probiotic cellulose was also effective against a methicillin-resistant *Staphylococcus aureus* strain. The synthesis of probiotic cellulose involves a single-step reaction under mild chemical conditions, thus cheaper and safer than the conventional methods to obtain bacterial cellulose.

1. Introduction

According to the World Health Organization (WHO), the increase of antibiotic-resistant bacteria is one of the biggest threats

* Corresponding author.
E-mail addresses: jmdl@ugr.es (J.M. Delgado-López), josema@ugr.es (J.M. Dominguez-Vera).

https://doi.org/10.1016/j.actbio.2021.01.039
1742-7061/

to global health [1]. Antibiotic resistance is responsible for around 700.000 deaths per year worldwide, with the potential to cause 10 million deaths by 2050 [1]. The WHO reported in 2014 that "a post-antibiotic era - in which common infections and minor injuries can kill - far from being an apocalyptic fantasy, is instead a very real possibility for the 21st century" [2]. New antibiotic-free approaches are thus urgently needed for the treatment and prevention of bacterial infections.

A promising alternative to antibiotics is the use of probiotics. Probiotics are live microorganisms traditionally known to help restore the natural balance of bacteria in the gut microbiota when it has been disrupted by an illness or treatment. Likewise, they may be helpful to prevent diarrhea when taking antibiotics and to ease some symptoms of irritable bowel syndrome. Nowadays, the term probiotic goes beyond commensal bacteria for the gut microbiota since probiotics can provide health benefits to other tissues, by restoring their corresponding microbiota and/or excreting antipathogenic compounds [3]. In particular, Lactobacilli strains have already shown antimicrobial properties and the ability to accelerate the healing process [4].

Nonetheless, non-encapsulated probiotics are vulnerable when nesting and proliferating in the hostile environment of the infected tissue, thus jeopardizing their viability and consequently their beneficial health effects [5]. Therefore, one of the keys to the use of probiotics is the choice of an appropriate matrix to host and protect them. However, most of the studies on engineering protective matrices for probiotics were intended for food and nutraceuticals [6–10] and very little has been done yet regarding the use of encapsulated probiotics to treat skin infections. The extra-protection and localization afforded by a matrix can reinforce the ability of the encapsulated probiotics to colonize and interact with the wound bed, facilitating the inhibition of the pathogenic growth process [4].

Bacterial cellulose (BC) is a biopolymer synthesized by some aerobic bacteria [11,12]. It has received special attention due to its unique properties in comparison with plant cellulose (PC). Both BC and PC consist of $\beta(1\rightarrow4)$ linked glucose units that self-assemble into fibers through a complex hierarchical process. However, BC is chemically pure, free of hemicellulose, lignin or pectin, and thus being nontoxic and biocompatible [11]. Furthermore, the thin nanofibers of BC, ranging from 40-80 nm in diameter, are approximately 100 times smaller than those of PC [13]. This confers BC higher surface area, notable mechanical properties, high water-holding capacity and high adsorption capability.

Thanks to these properties, BC has been widely studied for biomedical applications [14,15] and, in particular, for tissue engineering, reconstruction of damaged tissues [16], and as a wound dressing material [17–21]. BC provides optimum moisture balance to dry wounds, absorbs wound exudates, provides an effective physical barrier against external infection and does not adhere to the wound surface, thereby avoiding tissue damage upon removal [17,18]. Moreover, *in vivo* wound healing studies have demonstrated that BC-based materials feature faster epithelialization and regeneration than other commercially available products [12].

However, BC itself has no activity against bacterial infection, which is a recurrent issue affecting hard-to-heal chronic wounds. The synthesis of BC derivatives with antibacterial properties has long been, in fact, a challenge for biomaterial scientists. Most approaches dealt with BC functionalization by physical surface interactions or chemical bonding. Thus, antibacterial polymers, peptides or nanoparticles were incorporated to BC [22–26]. However, both physical and chemical approaches have limitations. BC contains available hydroxyl groups on its surface that facilitate the possibility of coating, but due to the weak interaction between BC and the coating, it potentially suffers from shedding. The chemical modification becomes difficult due to the poor solubility of BC, which makes necessary the use of solvents that influences the green safety of products, and limits its large-scale production.

BC has been recently functionalized with *Bacillus subtilis* resulting in a composite biomaterial with antimicrobial properties and the capacity of promoting skin wound healing [27]. However, the functionalization process required first the isolation and purification of BC and then the inoculation and further growth of the *bacillus*, which only penetrates few layers of the bacterial cellulose.

In this work, we have developed a one-pot approach under mild conditions to obtain antibiotic-free antibacterial biomaterials, so-called probiotic cellulose, which consist of cellulose films where probiotics progressively grow until completely invading the entire scaffold. Antibacterial assays (agar-diffusion and time-kill tests) demonstrated that probiotic cellulose is able to kill *Staphylococcus aureus (SA)* and *Pseudomonas aeruginosa (PA)*, the most active pathogens in severe skin infections and chronic wounds, even in pathogen-favorable media. Noticeably, probiotic cellulose was also found to be effective to inhibit the proliferation of methicillin-resistant *SA (MRSA)* isolated from clinical urine sample.

2. Materials and methods

2.1. Reagents and solutions

High-grade quality reagents were purchased from Sigma-Aldrich. Aqueous solutions were prepared with ultrapure water (18.2 MΩ.cm, Bacteria < 0.1 CFU/mL at 25 °C, Milli-Q, Millipore).

2.2. Bacterial strains and culture conditions

The lyophilized *Acetobacter xylinum* (ATCC 11142, *Ax*) was supplied by the Colección Española de Cultivos Tipo (CECT) and grown in Hestrin-Schramm (HS) [28] agar at 30 °C. *Lactobacillus fermentum* (*Lf*) and *Lactobacillus gasseri* (*Lg*) were kindly provided by Biosearch Life S.A. and grown in de Man, Rogosa and Sharpe medium (MRS, Oxoid) at 37°C.

The pathogenic strains of *Staphylococcus aureus* (CECT 976, *SA*) and *Pseudomonas aeruginosa* (CECT 108, *PA*) were supplied by the Colección Española de Cultivos Tipo (CECT). The pathogenic strains were grown in tryptic soy broth (TSB No2, Sigma-Aldrich) at 30°C and 37 °C, respectively.

MRSA bacteria were isolated from clinical urine sample at the Microbiology Laboratory of the "Virgen de las Nieves" University Hospital (Granada, Spain). The MicroScan system (Beckman Coulter, Brea, CA, USA) and mass spectrometry (Maldi-Tof®, Bruker Daltonik GmbH, Bremen, Germany) were used to identify the isolate. The MicroScan microdilution system was employed to characterize resistance to antibiotics. Minimum Inhibitory Concentration (MIC) assays were performed and the lowest concentration of the following antimicrobials (in mg mL^{-1}) was interpreted according to the EUCAST 2020 recommendations. The strain was found to be resistant to penicillin (>0.25), oxacillin (2), ciprofloxacin (>2), levofloxacin (>4), fosfomycin (64) and daptomycin (2); and susceptible to erythromycin (<0.5), clindamycin (<0.25), gentamicin (<1), vancomycin (2), teicoplanin (<1), mupirocin (<4), trimethoprim-sulfamethoxazole (<1/19), linezolid (2), rifampicina (<0.5) and tetracycline (<1). *MRSA* bacteria were grown in TSB at 36 °C.

2.3. Synthesis of bacterial cellulose (BC) and probiotic cellulose

The synthesis of probiotic celluloses (*Lf*- and *Lg*-cellulose) was carried out by co-culturing 0.1 mL of an *Ax* suspension (OD_{600nm} = 0.3) and 0.1 mL of a probiotic (*Lf* or *Lg*) suspension (OD_{600nm} = 0.4) in 1 mL of HS medium and aerobic conditions at 30 °C. The material obtained after 3 days of culture is referred to as bacterial cellulose (BC) in this work. Afterward, HS medium was

replaced by 5 mL of MRS and BC was incubated in an anaerobic atmosphere at 37 °C for 48 hours (Figure S1). The MRS medium was replaced after 24 hours. After 48 hours of culturing in MRS, probiotic-celluloses (*Lf*- or *Lg*-cellulose) were obtained.

With the aim of exploring the reproducibility of probiotic growth into the cellulose matrix, we performed three independent experiments with fresh batches of *Ax, Lf* or *Lg* and fresh solutions on different weeks obtaining 3 samples of *Lf*- and *Lg*-cellulose per batch. Subsequently, the probiotics into the matrix of each sample were quantified (see Section 2.6).

For the sake of comparison, bacterial cellulose was also purified and then functionalized with probiotics. The purification of BC was achieved as follows: immersion in ethanol, boiling in water for 40 min, immersion in NaOH 0.1M at 90 °C for 1 hour (with four dissolution replacements), and neutralization in distilled water. Cellulose was then functionalized with adsorbed probiotics by incubation in MRS broth inoculated with *Lf* (BC+*Lf*) or *Lg* (BC+*Lg*), at the same conditions as probiotic celluloses.

Lf and *Lg* are included in the list of Qualified Presumption of Safety (QPS) of the European Food Safety Authority (EFSA) and Food and Drug Administration (FDA). QPS provides a safety status for microorganisms intentionally used in the food and feed chain. These microorganisms can be also used as living entities that may reach the consumer as such, or may be used as production organisms or as dead biomass [29]. Likewise, FDA approved some wound dressing devices based on bacterial cellulose [15,30].

2.4. Gram staining

This staining protocol allows differentiating between two major bacterial groups, Gram-positive (stained purple) and Gram-negative (stained red) cells. *Ax* is a Gram-negative bacterium, whereas *Lf* and *Lg* are Gram-positive bacteria. After 1, 2 and 7 days of incubation in MRS, *Lf*-cellulose was dehydrated in gradient ethanol and washed with xylene [31]. Then, the samples were embedded in paraffin and transversally cut in 4 μm sections using a microtome. Slides were deparaffinized, cleared in xylene, and rehydrated before the staining. Then, a standard Gram staining protocol was performed. In brief, crystal violet was applied for 1 minute at room temperature, and slides were briefly rinsed under running water to remove the excess of staining. Iodine mordant was applied for 30 seconds and washed with water. To remove violet crystal from Gram-negative bacteria, slides were covered with ethanol for 15 seconds and quickly rinsed under running water until the water run clear. Finally, Gram-negative bacteria were stained with safranin for 1 minute and rinsed with water. The slides were observed using an iScope (Euromex) microscope, in bright field mode and under a 100x immersion oil objective to differentiate between Gram-positive and Gram-negative. The same slides were also observed using a Nikon Eclipse E200 microscope, in dark field mode and under a 10x objective to obtain macroscopic images of the whole *Lf*-cellulose section. Images were acquired with an AxioCam ERc 5s (ZEISS) camera.

2.5. Field emission scanning electron microscopy (FESEM)

Probiotic celluloses were fixed in 1 mL of cacodylate buffer (0.1 M, pH 7.4) containing 2.5% of glutaraldehyde at 4 °C for 24 h. Subsequently, samples were washed with cacodylate buffer three times for 30 min at 4 °C. The samples were stained with osmium tetroxide (OsO_4) solution (1 % v/v) for 2 h in the dark, being then repeatedly rinsed with Milli-Q water to remove the excess of OsO_4 solution. Samples were then dehydrated at room temperature with ethanol/water mixtures of 50%, 70%, 90% and 100% (v/v) for 20 min each, being the last concentration repeated three times and dried at the CO_2 critical point. Finally, dehydrated samples were mounted on aluminum stubs using a carbon tape, sputtered with a thin carbon film, and analyzed using a FESEM (Zeiss SUPRA40V) of the Centre for Scientific Instrumentation (University of Granada, CIC-UGR). The fiber width distribution of each condition was obtained by measuring 100 fibers of different SEM micrographs with ImageJ software (version 1.48v; NIH, Bethesda, MD).

2.6. Quantification of immobilized probiotics

Probiotic cellulose (2 cm-diameter, 1.5 mm-thick) was digested with cellulase from *Trichoderma reesei* (No C2730-50ML, Sigma–Aldrich). For this purpose, samples were immersed in 2 mL of enzyme solution (50 μL cellulase/mL potassium phosphate buffer, 50 mM, pH 6) and incubated at 37 °C for 1h, with orbital shaking (180 rpm) [32]. Then, the samples were centrifuged to collect the probiotics and washed three times with saline solution. Probiotics were suspended in 5 mL of saline solution and colony-forming units (CFU) were determined by counting in MRS-agar plates after 24 h of incubation at 37 °C in anaerobic conditions (using the BD GasPak^{TM} ES Anaerobe Container System). The serial dilution with a number of visible colonies around 20-300 was used to calculate CFU, and plating was performed in triplicate. Nine independent samples of probiotic cellulose (*Lf*- or *Lg*-cellulose) were digested and analyzed. Data are expressed as mean of experimental replicates (n = 9) ± standard deviations.

The mass of BC was weighted to denote the concentration of probiotics as CFU per milligram of cellulose. To this aim, samples were immersed in ethanol after the co-culture in HS medium (aerobiosis), boiled in deionized water for 30 min, treated with 0.1 M NaOH at 90 °C for 1h, and washed with deionized water until neutral pH was achieved [33]. With this treatment, BC was purified and bacteria were removed. Finally, purified celluloses were dried at 100 °C and weighted using a BOECO BAS31plus microbalance. Three replicates were measured.

2.7. Live-dead viability assays

Bacterial viability of BC and probiotic celluloses was qualitatively assessed by confocal laser scanning microscopy (CLSM). The samples were washed with sterile saline solution and stained with LIVE/DEAD BacLight Bacterial Viability Kit (ThermoFisher) following the manufacturer's instructions. This assay combines membrane-impermeable DNA-binding stain, i.e. propidium iodide (PI), with membrane-permeable DNA-binding counterstain, SYTO9, to stain dead and live and dead bacteria, respectively. Cell viability along the BC matrix was evaluated with a confocal microscope (Nikon Eclipse Ti-E A1, CIC-UGR) equipped with a 20x oil immersion objective. For acquiring SYTO 9 signals (green channel), 488 nm laser and 505–550 nm emission filter were used. For PI (red channel), 561 nm laser and 575 nm long-pass emission filter were used. Images were analyzed with NIS Elements software.

2.8. Bacterial activity

The metabolic activity of the two probiotic celluloses, *Lf* and *Lg*-cellulose, freshly prepared and stored for one week or one month at 25 and 4 °C was evaluated by pH monitoring (HACH SensIONTM pHmeter). Probiotic pellets obtained after the digestion of probiotic celluloses were also stored in the same conditions for comparison. The reductive capacity against electrochromic polyoxometalates (POM, $[P_2Mo^{VI}{}_{18}O_{62}]^{6-}$) was evaluated according to a previously reported protocol [34]. Briefly, *Lf*-cellulose and *Lg*-cellulose samples were incubated in 100 mL of diluted MRS broth (1:10) in anaerobic conditions, at 37 °C and 180 rpm. At scheduled times (0, 1, 2, 4, 5, 7 and 20 h), 1mL-aliquot was collected, centrifuged (3000 g, 5 min) and filtered with a 0.2 µm filter to remove any residual

bacteria. Then, 190 μL of the sample was mixed with 10 μL of POM solution (10 mM) on a 96-well and irradiated with UV light (365 nm) for 10 min. The absorbance at 820 nm was measured in a Tecan's NanoQuant plate reader (CIC-UGR). Data are expressed as mean of experimental replicates (n = 3) ± standard deviations.

2.9. Inhibitory and antimicrobial activity against SA, PA and MRSA

The antimicrobial activity of non-encapsulated probiotics against *SA* and *PA*, two common pathogens involved in wound infection, was initially evaluated by an agar spot test in MRS [35]. In brief, overnight cultures of probiotics (10^9 CFU mL^{-1}) were inoculated as a 5 µL spot on MRS agar plates (3 spots/plate). After 24 h of incubation at 37 °C under anaerobic conditions, the plates were overlaid with 6 mL of TSA (0.7 % w/v agar) at 45 °C, previously inoculated with 0.1 mL of an overnight culture of *SA* or *PA*. The plates were incubated 24 h at 30 °C and 37 °C, respectively, before examination of the corresponding inhibition zones.

Subsequently, the antimicrobial activity of probiotic cellulose was evaluated by agar diffusion assays [36] but in pathogen-favorable tryptic soy media [37]. The agar diffusion assay was carried out as follows: 0.1 mL of an overnight culture of *SA, PA or MRSA* was spread on petri dishes containing TSA. Then, *Lf*- or *Lg*-cellulose were placed on agar plates containing the selected bacterial strains and incubated 24 hours at pathogen optimal temperature (37 °C for *PA*, 30 °C for *SA* and 36 °C for *MRSA*) before examination of inhibition zones. Aliquots of the inhibition zones were selectively grown in MRS or TSB media. In the experiment with *SA*, we only found proliferation in MRS, pointing out the presence of some probiotic cellulose detachment (see Fig. 6B). Control experiments with non-encapsulated probiotics, bacterial cellulose (BC) and cellulose with adsorbed probiotics (BC+*Lf*, BC+*Lg*) were also carried out following the same protocol and using equivalent CFU of *Lf* and *Lg*. After 24 hours of incubation, the inhibition zones of non-encapsulated probiotics and celluloses were imaged and compared.

The inhibitory activity of probiotic cellulose was evaluated by time-kill assays. *Lg*- and *Lf*-cellulose were introduced into TSB medium containing 7×10^6 CFU of pathogen and incubated with orbital shaking for 24 h at 30 °C for *SA* and at 37 °C for *PA* [38,39]. The pathogen survival was assayed by the serial dilution method, plating on TSA in triplicate and counting after 24 hours of incubation. Control experiments with bacterial cellulose (BC) were also carried out following the same protocol.

2.10. Statistics

Results were analyzed with the software GraphPad Prism 5 and data are expressed as mean ± standard deviation. For the statistical analysis, we applied the one-way ANOVA, Bonferroni's method.

3. Results

3.1. Synthesis and characterization of probiotic cellulose

The synthetic approach used to obtain probiotic cellulose is represented in Fig. 1. It is based on the fact that cellulose-producing bacterium *Ax* is strictly aerobic, while probiotics are facultative anaerobic bacteria (Fig. 1A and S1). Two types of probiotics, selected according to their activity in terms of the prevention and/or treatment of infections [40,41], were explored. Specifically, *Lf* is an immunostimulant that strengthens the microbiota and *Lg* has exhibited antimicrobial activity against *SA* [40], one of the most common bacteria involved in chronic skin ulcers [42].

The co-culture of *Ax* and probiotic in an aerobic HS medium (optimum for *Ax*) resulted in the formation of a thick cellulose film (Figure S1) containing *Ax* and the corresponding probiotic (*Lf* or *Lg*). Gram staining shed light on the growth of probiotic cellulose (Fig. 2 and S2), since *Ax* and probiotics are Gram-negative and Gram-positive bacteria, respectively (Figure S2). Under aerobic conditions, the facultative anaerobic probiotics were situated at the bottom of the cellulose film (Fig. 2A), that is, as far away as possible from the air–culture interface. Replacing the HS with MRS medium and removing oxygen (anaerobic conditions are optimal for probiotics) caused the massive proliferation of probiotics (Fig. 2B), which completely invaded the cellulose network (Fig. 2C).

BC produced aerobically in the presence of *Ax* and probiotic is, therefore, a two-sided material. FESEM micrographs of the air-exposed face showed the typical fibrous morphology of *Ax* (Fig. 3A and Figure S3), whereas bacteria at the submerged face presented the typical bacilliform appearance of probiotics. In fact, FESEM micrographs of the cross-section (Fig. 3B) revealed two clearly differentiated areas: one exposed to air, containing exclusively *Ax*, and the other exposed to the bulk aqueous phase, which only included probiotics. When increasing the incubation time in the anaerobic medium, the probiotics extensively proliferated and invaded the entire cellulose matrix to such an extent that both faces were similar (Fig. 3C and S3). Under these latter conditions no evidences of reminiscent *Ax* were detected, while probiotics were distributed throughout the cellulose network. Despite the high density of probiotics (Fig. 3C), *i.e.*, $1.4 \times 10^{11} \pm 3.1 \times 10^{10}$ and $8.7 \times 10^{10} \pm 1.5 \times 10^{10}$ CFU of *Lf* and *Lg*, respectively, per mg of cellulose, the entrapment did not affect the size of the cellulose nanofibers, which maintained diameters ranging between 20 and 90 nm (Figure S4). The high number of entrapped probiotics modifies the optical properties of probiotic cellulose in comparison to cellulose film grown under aerobic conditions (Fig. 3D).

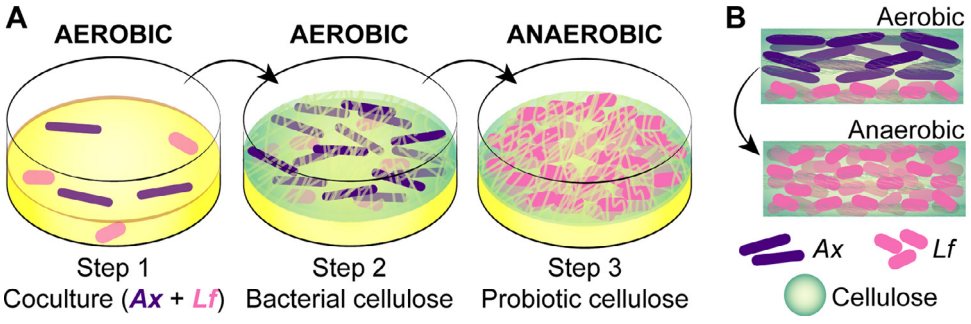

Fig. 1. Graphical sketch of the protocol used to obtain probiotic cellulose. The co-culture of *Ax* and the probiotics (*Lf* or *Lg*, step 1) under aerobic conditions produces a thick bacterial cellulose gel (BC, step 2), which, under anaerobic conditions, is gradually invaded by probiotics resulting in probiotic cellulose (step 3). (B) Graphical representation (cross-section) of BC obtained under aerobic conditions (top, step 2) and probiotic cellulose produced by switching to anaerobic conditions (bottom, step 3).

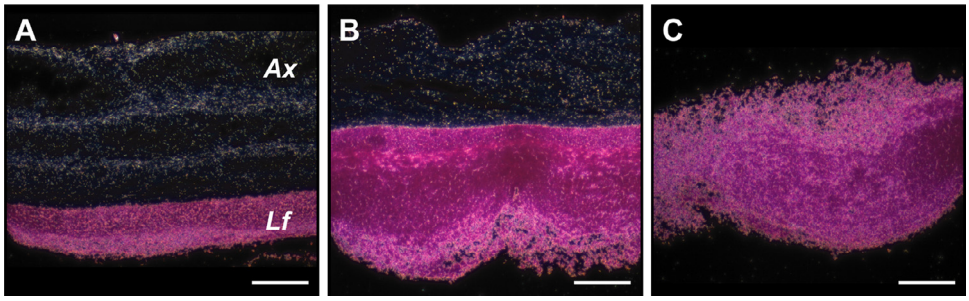

Fig. 2. Dark-field optical micrographs of cross-sections of Gram-stained cellulose films showing the gradual invasion of the probiotics as a function of increasing incubation time (from left to right). Scale bar = 100 µm.

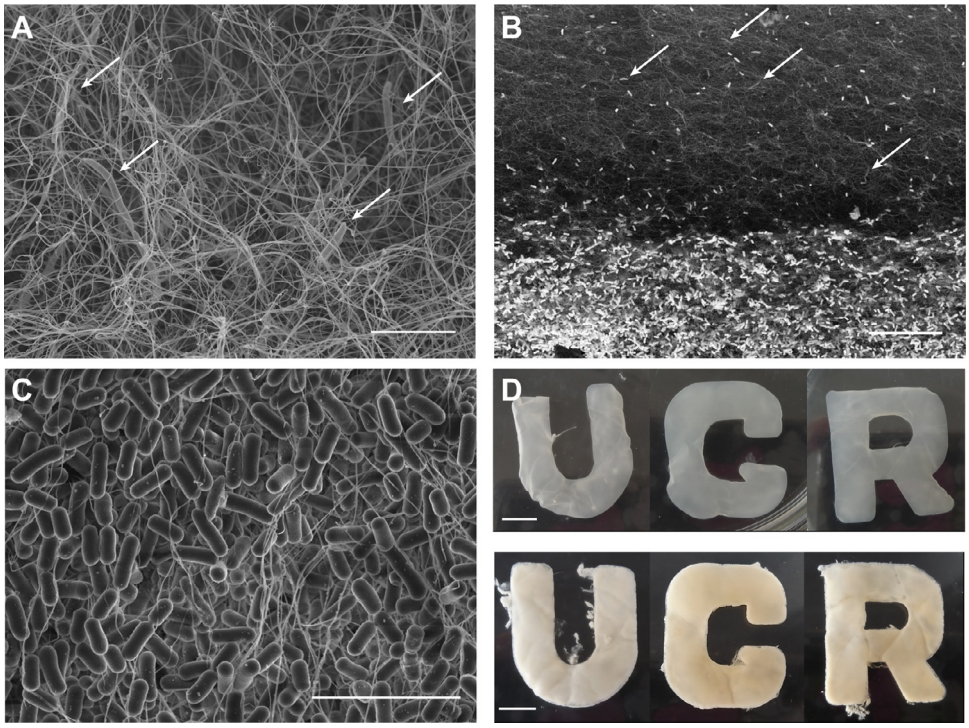

Fig. 3. (A) FESEM micrograph of the air-exposed surface of cellulose co-cultured with *Ax* and *Lf* in aerobic conditions. Note that most of the bacteria present the typical fibrous morphology of *Ax* (white arrows). (B) FESEM micrograph of the cross-section of the two-sided biomaterial formed under anaerobic conditions (24 h of incubation): one side contains *Ax* (white arrows) and the other *Lf*. (C) FESEM micrograph of the surface of cellulose co-cultured with *Ax* and *Lf* under anaerobic conditions (48 h of incubation). In this case, both surfaces (exposed to either air or solution) appeared fully covered of bacteria exhibiting the typical morphology of *Lf*. Scale bars (A,C) = 5 µm; (B)= 20 µm. (D) Photographs of BC (top) and probiotic cellulose (bottom). Scale bar = 1 cm.

3.2. In vitro *live-dead viability*

Live/dead viability tests, based on SYTO^{TM} 9 and propidium iodide fluorescent dyes, demonstrated that the probiotics entrapped in the cellulose remained viable (Fig. 4). Confocal laser scanning microscopy (CLSM) images of the cellulose obtained after co-culture of *Ax* and *Lf* in aerobiosis contained a mixture of green spots (live) with a high density of red spots (dead) of fibrous *Ax* and shorter bacilliform *Lf* bacteria (Fig. 4A-D). Contrastingly, the probiotic cellulose showed a very high density of live probiotics (green spots), with very few red spots (dead) (Fig. 4G-J). Moreover, the 3D CLSM image confirmed that probiotic cellulose is a homogeneous material, since live probiotics migrated and colonized the entire cellulose matrix after 48 h (Fig. 4K-L).

3.3. Activity assays

Importantly, the entrapped probiotics were also metabolically active. Live *Lf* and *Lg* excrete metabolites to the medium, in particular lactic acid, which regulates the pH at around 4. Within a few hours, the pH of the MRS media in contact with the probiotic cellulose (both *Lf*- and *Lg*-cellulose) dropped from 7 to approximately 4, a value very close to the pk_a of lactic acid (Fig. 5A), confirming that probiotics within the cellulose matrix retain their metabolic activity.

In addition, we assessed the metabolic activity of probiotic cellulose using an assay previously developed by our team, that correlates the reductive capacity of bacteria to their metabolic activity, using an electrochromic polyoxometalate (POM) [34,43]. Once reduced, POM exhibits an absorption band in the UV-vis spectrum centered at 820 nm. The evolution of this absorption band after incubating aliquots from the supernatants of probiotic cellulose with an aqueous solution of POM was monitored (Fig. 5B). The increase of the absorbance at 820 nm supports the activity of probiotics in probiotic cellulose.

3.4. Activity assays of probiotics after long-time storage

The probiotic activity of *Lf*- and *Lg*-cellulose after storage at 4 and 25 °C for one week and one month was analyzed by the time

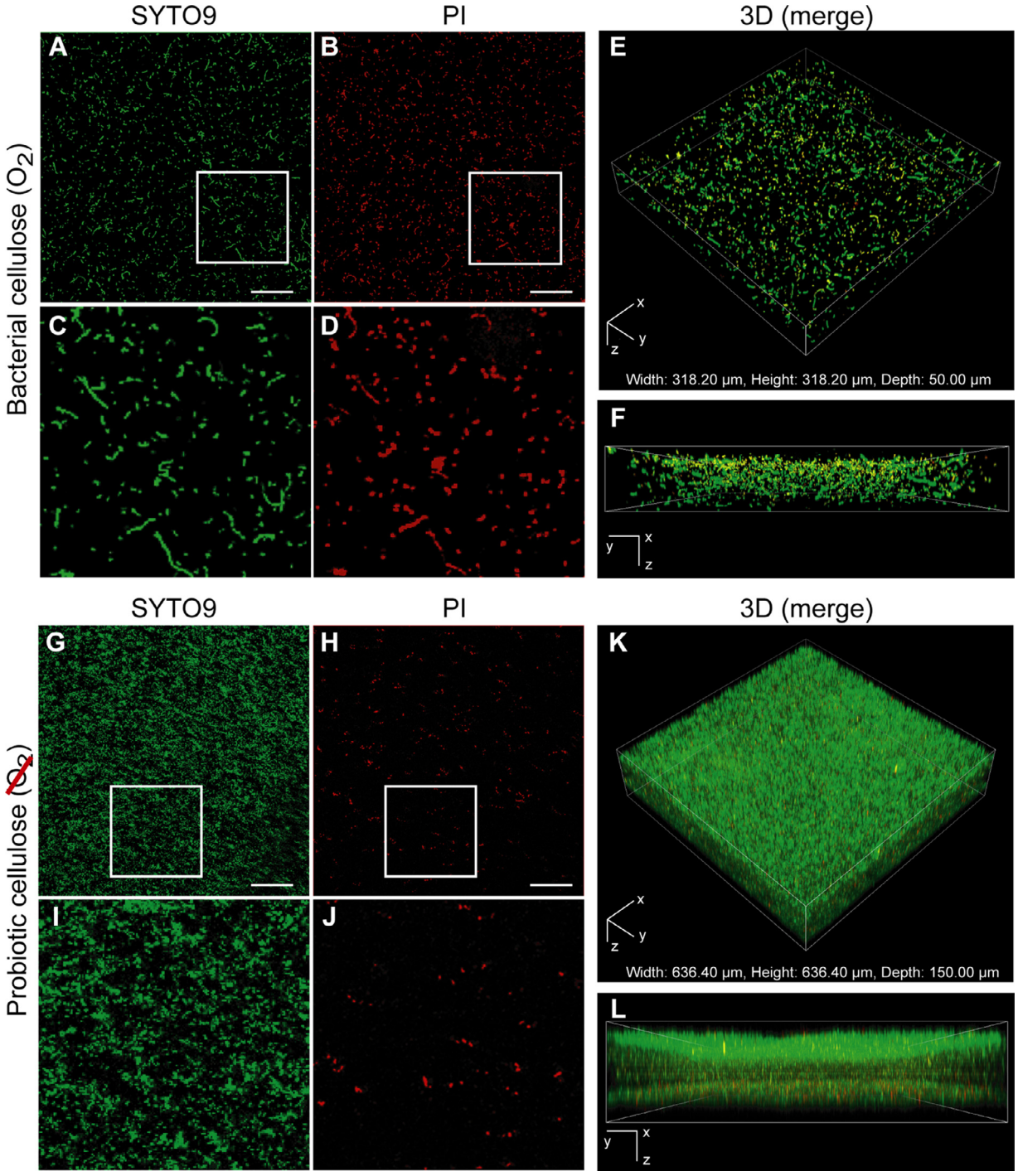

Fig. 4. CLSM images of BC co-cultured with *Ax* and *Lf* under aerobic, (A-F), and then, anaerobic conditions, (G-L). Green channel (SYTO 9, live bacteria), red channel (propidium iodide, dead bacteria) are shown. Panels (C, D) and (I, J) correspond to expanded views of the boxes (3x) in images (A, B) and (G, H), respectively. The 3D maps are representative of the merged channels (live and dead). Scale bars = 50 µm.

evolution of pH in MRS media. The results were compared to those of non-encapsulated *Lf* and *Lg* (Figure S5). The activities of *Lf*- and *Lg*-cellulose were similar to those of free probiotics after one week of storage, both at 4 and 25 °C, reaching a pH value of 4 after 25 hours in MRS cultures. However, significant differences were observed after one month of storage. While the activity of *Lf* and *Lf*-cellulose kept similar at 4°C, it became drastically different when the storage for one month was carried out at 25 °C. At this temperature, the extra-protection effect of the cellulose on the probiotic activity was evident, since free *Lf or Lg*, in contrast to *Lf*- or *Lg*-cellulose, did not reach the pH 4 after 25 hours in MRS.

3.5. Inhibitory and antimicrobial activity

The antibacterial activity of probiotic cellulose was assessed against *SA* and *PA*, two opportunistic pathogens responsible for a broad range of skin infections, some of which are potentially fatal (severe and chronic wounds) [42,44]. Both *Lf* and *Lg* have shown antimicrobial activity against *SA* and *PA* in media that favor the proliferation of probiotics [40,44] (Figure S6A). However, we found that neither *Lf* nor *Lg* could inhibit the growth of *SA* or *PA* in optimal pathogenic media such as TSA (Figure S6B). This subtle nuance is of paramount importance, because in a real-life infection sce-

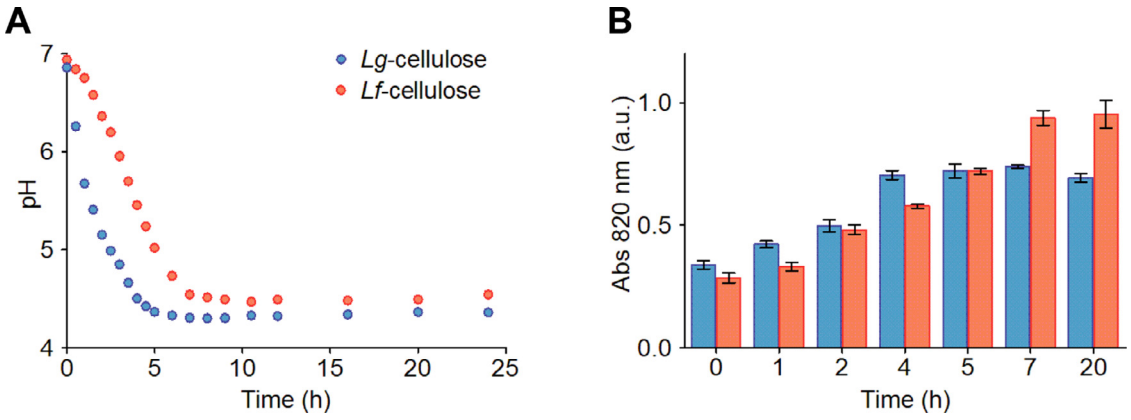

Fig. 5. (A) Time evolution of the pH of MRS media containing a film of probiotic (*Lf* or *Lg*) cellulose. (B) Time dependence of the UV-vis absorbance at 820 nm of probiotic cellulose in contact with a solution-containing POM. Data are expressed as mean with the corresponding standard deviation as error bars.

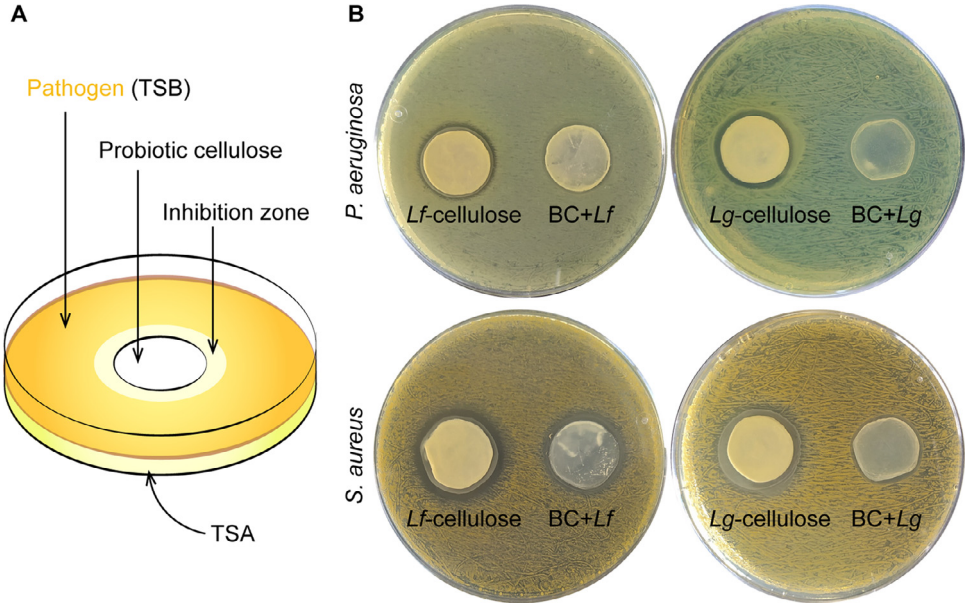

Fig. 6. Inhibitory activity of probiotic cellulose. (A) Diagram of the experimental protocol used to assess the inhibitory activity (B) of probiotic cellulose (*Lf*- and *Lg*-cellulose) and BC with adsorbed probiotics (BC+*Lf* and BC+*Lg*) against *SA* and *PA*.

nario, the pathogen and probiotic meet in an environment that is optimal for the former but not for the latter. With this in mind, we tested the antibacterial activity of probiotic cellulose using the agar diffusion experiments depicted in Fig. 6A, where the pathogens were dispersed in TSA. Even in these unfavorable conditions, probiotic celluloses (with *Lf* and *Lg*) produced inhibition zones against both pathogens (Fig. 6B). Noticeably, under these unfavorable conditions for probiotics, BC functionalized with *Lf* or *Lg* through an "adsorption-incubation" procedure (BC+*Lf* or BC+*Lg*) as that proposed by Digel *et al.* [27] did not inhibit in the same extent the pathogenic proliferation in TSA media (Fig. 6B).

These observations were confirmed by time–kill experiments. When *SA* or *PA* were cultivated in TSB (an unfavorable medium for probiotics) [38,45], we found pathogen proliferation, from initial loads of 10^6–10^7 to 10^9 CFU after 24 h (Fig. 7A). In a control experiment, we observed that the addition of bacterial cellulose did not affect the pathogen proliferation (Fig. 7A, *SA*+BC or *PA*+BC bars). Nonetheless, when probiotic cellulose (either *Lf*- or *Lg*-cellulose) was added instead of bacterial cellulose, an important decrease of pathogen viability was observed. In particular, *Lf*-cellulose inhibited *PA* and *SA* growth after 24 hours, while *Lg*-cellulose practically killed *PA* and notably decreased *SA* viability (Fig. 7B).

These interesting findings motivated us to explore the activity of probiotic cellulose against *MRSA* by agar diffusion assays. As found in Fig. 8, both *Lf*- and *Lg*-cellulose inhibited the growth of *MRSA*. Although some inhibitory effects were also found for BC+*Lf* and BC+*Lg* (biomaterials prepared by an adsorption-incubation procedure), the inhibition zones were smaller than those found for probiotic celluloses (Fig. 8).

4. Discussion

Although BC is one of the most widely studied biomaterials for biomedical applications [14,15] and, in particular, as a wound dressing [17–21], it has no activity against bacterial infections. In addition, the isolation of BC and/or its derivatives requires a long and expensive procedure involving successive treatments with ethanol and/or alkali at high temperatures, to eliminate any remnants of cellulose-producing bacteria [25–27, 33, 46–48].

Probiotic-containing bacterial cellulose was recently achieved by incubation of BC (previously purified) in a culture of *Bacillus subtilis* [27]. Following this "adsorption-incubation" methodology, the *bacillus* only penetrates a few layers of the bacterial cellulose. Likely, the dense cellulose network does not allow the penetra-

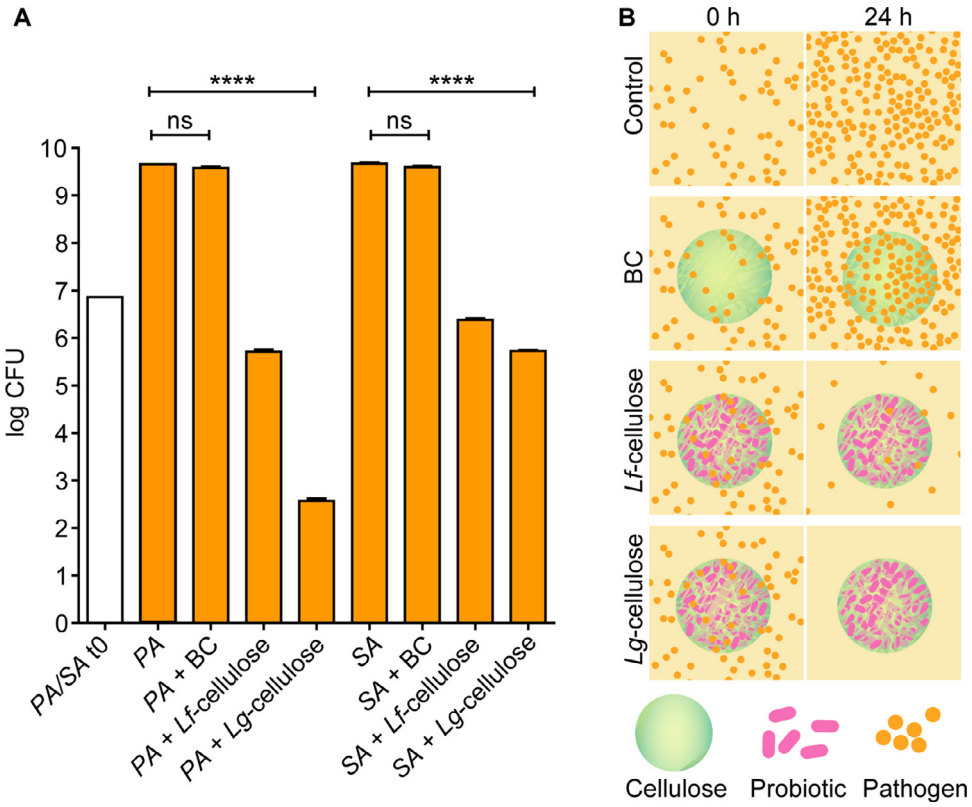

Fig. 7. Antibacterial activity of probiotic cellulose. (A) *PA* and *SA* survival after co-incubation with BC or probiotic celluloses (*Lf*- and *Lg*-cellulose) in TSB. Asterisks and ns denote statistical significance ($p < 0.001$) and no significance, respectively. (B) Diagram depicting the bactericidal properties of *Lf*- and *Lg*-cellulose compared to the corresponding control assays.

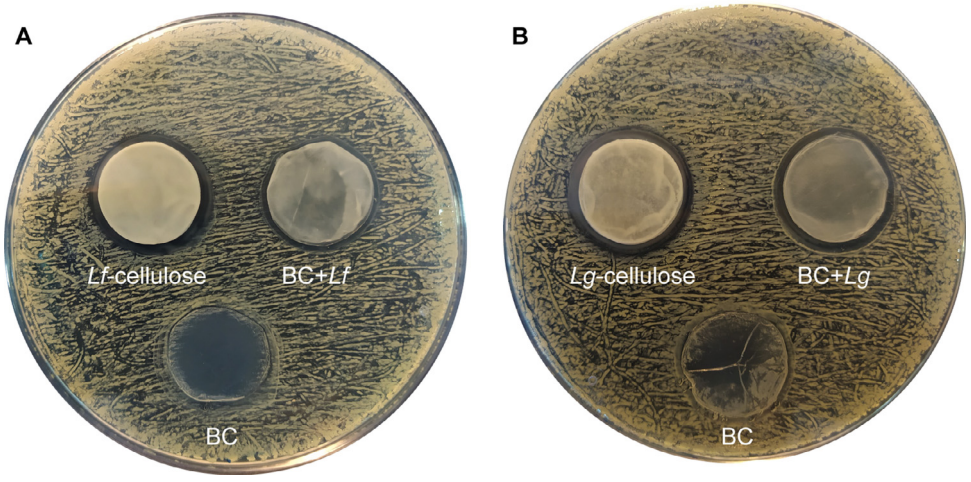

Fig. 8. Inhibitory activity of probiotic cellulose (A, *Lf*-cellulose and B, *Lg*-cellulose) against *MRSA* by agar diffusion tests on TSA plates. BC+*Lf* (A), BC+*Lg* (B) and pure BC were also tested. Even though the media was optimal for the pathogens, clear inhibition zones appeared around the probiotic cellulose and in a less extent around the biomaterials prepared through an adsorption-incubation procedure (BC+*Lf* and BC+*Lg*).

tion of the *bacillus* to the porous cellulose network. SEM images showed the presence of *bacillus* adhered to the bacterial cellulose surface. The one-pot strategy here reported clearly improves the integration of probiotics into the entire BC matrix. BC was grown into an optimum probiotic culture (under anaerobic conditions) (Fig. 1 and S1), which allowed probiotics to fully invading the under-construction cellulose scaffold (Fig. 4K-L). As a result, our biomaterial, probiotic cellulose, incorporated a much higher amount of bacteria (ca. 10^{14} CFU per g of BC) in comparison to that obtained by the "adsorption-incubation" procedure (10^{10} CFU of *bacillus* were incorporated per g of BC) [27]. Moreover, our strategy, in contrast to that reported by Digel *et al.* [27] does not require the purification and isolation of bacterial cellulose films. Probiotic cellulose is in fact the first bacterial cellulose derivative that does not require the previous isolation of bacterial cellulose. This aspect is of the utmost importance when considering the economic and environmental factors associated with the large-scale production of cellulose-based materials.

The retention of high metabolic and cellular activities is another critical parameter for the successful use of probiotic cellulose for the treatment of bacterial infections. The probiotics in probiotic cellulose are alive (Fig. 4) and metabolically active (Fig. 5).

At the same time, the matrix provides the probiotics with extra-protection. In fact, the probiotic activity of probiotic cellulose, in contrast to non-encapsulated probiotics, is maintained after one-month storage at room temperature or 4 °C. This extra-protection is of high relevance for real applications and confirms the suitability of bacterial cellulose as a matrix for the long-term stabilization of alive and active probiotics.

Although many studies have tried to develop effective vaccines or treatments against *SA* and *PA*, none of them have so far gained approval from regulatory authorities, which makes the development of antibacterial treatments against these bacteria even more significant. Interestingly, probiotic cellulose has shown excellent antibacterial properties (bacteriostatic and bactericidal) against *SA* and *PA*, even in media where the pathogens commonly proliferate (Fig. 6). However, the biomaterial made by an "adsorption-incubation" procedure [27], containing the same components, *i.e.* bacterial cellulose and the same probiotics (BC+*Lf* or BC+*Lg*), showed little or no inhibition of the pathogenic proliferation (Fig. 6B). This difference suggests that the antibacterial activity of *Lf*- and *Lg*-cellulose is mainly due to the high population of encapsulated probiotics and not to the adsorbed ones, as those present in BC+*Lf* or BC+*Lg*, obtained by the "adsorption-incubation" procedure [27]. The health benefits of probiotics are well demonstrated but, unfortunately, little is yet known about their mechanisms of action. Our results did not provide insights on the identification of excreted species of probiotic cellulose leading to the inhibition of pathogenic growth. However, we can confirm that the observed inhibitory effects are intrinsic to the probiotics since bacterial cellulose has no antibacterial activity (Fig. 6). In contrast to the conventional molecular approach by which antibiotics or antibacterial species are promptly delivered, probiotics act as antibacterial bombs that produce a continuous release of antibacterial species while remaining alive.

Once the antibacterial properties of probiotic cellulose were demonstrated against the two most common strains in skin infections (*SA* and *PA*), we took a further step to prove that probiotic cellulose also inhibited the proliferation of an antibiotic-resistant strain, such as *MRSA,* which has shown resistance or susceptibility to a large variety of antibiotics (Section 2.2). Both *Lf*- and *Lg*-cellulose resulted active against *MRSA*, leading to larger inhibition zones than those produced by BC+*Lf* or BC+*Lg*, pointing out once more the higher antibacterial activity of probiotic cellulose with respect to those made by the "adsorption-incubation" procedure. Further work is in progress to develop probiotic celluloses that simultaneously contain both *Lf* and *Lg*, or probiotic cocktails, with the aim to study an eventual probiotic synergy as a strategy to improve the antibacterial properties.

5. Conclusions

We have developed a new antibiotic-free antibacterial biomaterial – probiotic cellulose – which consists of bacterial cellulose loaded with live and active probiotics. The two probiotic celluloses (*Lg*- and *Lf*-cellulose) showed enhanced antibacterial activity against *SA* and *PA*, the two most active pathogens in severe skin infections, and methicillin-resistant *MRSA*. Furthermore, probiotic celluloses, in contrast to non-encapsulated probiotics, exhibit antibacterial efficacy even in conditions that are favorable for pathogens and unfavorable for probiotics. Our strategy to produce probiotic cellulose can be extended to other facultative anaerobic probiotics or even combining different probiotics or other active species such as nanoparticles, polymers or peptides with the aim of obtaining multifunctional biomaterials towards other complex microbial infections. Moreover, the production of probiotic cellulose involves a single-step process under mild conditions and does not require the lengthy and expensive chemical treatments necessary to isolate bacterial cellulose, and thus can be easily scaled for industrial production. Probiotic cellulose is an antibiotic-free antibacterial agent with practical application today, and tomorrow, in a hypothetical post-antibiotic era, where common infections and minor injuries could kill.

Statement of significance

Antibiotic resistance is responsible for around 700.000 deaths per year worldwide, with the potential to cause 10 million deaths by 2050. New antibiotic-free approaches are thus urgently needed for the treatment and prevention of bacterial infections. We produced probiotic cellulose, which consists of dense films of cellulose nanofibers completely invaded by live and metabolically active probiotics. This antibiotic-free biomaterial exhibited excellent anti-bacterial activity against *Staphylococcus aureus* and *Pseudomonas aeruginosa*, the most active pathogens in skin infections and chronic wounds. Likewise, probiotic cellulose was also effective against a methicillin-resistant *Staphylococcus aureus* strain. The synthesis of probiotic cellulose involves a single-step reaction under mild chemical conditions, thus cheaper and safer than the conventional methods to obtain bacterial cellulose.

Declaration of Competing Interest

The authors declare that they have no known competing financial interests or personal relationships that could have appeared to influence the work reported in this paper.

Acknowledgements

This work was funded by the Spanish Ministerio de Ciencia, Innovación y Universidades (MICIU) (projects FEDER PID2019-111461GB-I00 and *Ramón y Cajal* RYC-2016-21042). L.S. and G.B.R.-R. acknowledge the Spanish MICIU for the predoctoral contract within the FPU program (FPU16/01360) and the postdoctoral contract within the Juan de la Cierva Program (JdC-2017), respectively. We heartily thank Prof. Manuel Martínez Bueno (Department of Microbiology, University of Granada) and Prof. Anna Roig (Institut de Ciència de Materials de Barcelona, ICMAB-CSIC) for fruitful discussions. The authors also thank the "Unidad de Excelencia Química aplicada a Biomedicina y Medioambiente" (UGR) for funding and support. The courtesy of the scientific and technical staff of the Center for Scientific Instrumentation (CIC, University of Granada), Ana Santos, Concepción Hernández and Isabel Guerra, is heartily acknowledged.

Supplementary materials

Supplementary material associated with this article can be found, in the online version, at doi:10.1016/j.actbio.2021.01.039.

References

[1] C. Willyard, The drug-resistant bacteria that pose the greatest health threats, Nature 543 (2017) 15.
[2] W.H. Organization, Antimicrobial Resistance: Global Report on Surveillance, World Health Organization, 2014.
[3] C. Vuotto, F. Longo, G. Donelli, Probiotics to counteract biofilm-associated infections: promising and conflicting data, Int. J. Oral Sci. 6 (2014) 189.
[4] C.G. Tsiouris, M.G. Tsiouri, Human microflora, probiotics and wound healing, Wound Med. 19 (2017) 33–38.
[5] M. Saarela, G. Mogensen, R. Fondén, J. Mättö, T. Mattila-Sandholm, Probiotic bacteria: safety, functional and technological properties, J. Biotechnol. 84 (2000) 197–215.
[6] M.J.M. Villena, F. Lara-Villoslada, M.A.R. Martínez, M.E.M. Hernández, Development of gastro-resistant tablets for the protection and intestinal delivery of Lactobacillus fermentum CECT 5716, Int. J. Pharm. 487 (2015) 314–319.
[7] T. Huq, C. Fraschini, A. Khan, B. Riedl, J. Bouchard, M. Lacroix, Alginate based nanocomposite for microencapsulation of probiotic: effect of cellulose nanocrystal (CNC) and lecithin, Carbohydr. Polym. 168 (2017) 61–69.

[8] P. Singh, S. Magalhães, L. Alves, F. Antunes, M. Miguel, B. Lindman, B. Medronho, Cellulose-based edible films for probiotic entrapment, Food Hydrocoll. 88 (2019) 68–74.
[9] P. Singh, B. Medronho, T. dos Santos, I. Nunes-Correia, P. Granja, M.G. Miguel, B. Lindman, On the viability, cytotoxicity and stability of probiotic bacteria entrapped in cellulose-based particles, Food Hydrocoll. 82 (2018) 457–465.
[10] J. Burgain, C. Gaiani, M. Linder, J. Scher, Encapsulation of probiotic living cells: from laboratory scale to industrial applications, J. Food Eng. 104 (2011) 467–483.
[11] R.J. Moon, A. Martini, J. Nairn, J. Simonsen, J. Youngblood, Cellulose nanomaterials review: structure, properties and nanocomposites, Chem. Soc. Rev. 40 (2011) 3941–3994.
[12] H. Ullah, F. Wahid, H.A. Santos, T. Khan, Advances in biomedical and pharmaceutical applications of functional bacterial cellulose-based nanocomposites, Carbohydr. Polym. 150 (2016) 330–352.
[13] P.R. Chawla, I.B. Bajaj, S.A. Survase, R.S. Singhal, Microbial cellulose: fermentative production and applications, Food Technol. Biotechnol. 47 (2009) 107–124.
[14] G.F. Picheth, C.L. Pirich, M.R. Sierakowski, M.A. Woehl, C.N. Sakakibara, C.F. de Souza, A.A. Martin, R. da Silva, R.A. de Freitas, Bacterial cellulose in biomedical applications: a review, Int. J. Biol. Macromol. 104 (2017) 97–106.
[15] S. Gorgieva, Bacterial cellulose as a versatile platform for research and development of biomedical materials, Processes 8 (2020).
[16] W.K. Czaja, D.J. Young, M. Kawecki, R.M. Brown Jr, The future prospects of microbial cellulose in biomedical applications, Biomacromolecules 8 (2007) 1–12.
[17] I. Anton-Sales, U. Beekmann, A. Laromaine, A. Roig, D. Kralisch, Opportunities of bacterial cellulose to treat epithelial tissues, Curr. Drug Targets. 20 (2019) 808–822.
[18] W. Czaja, A. Krystynowicz, S. Bielecki, R.M. Brown Jr, Microbial cellulose—the natural power to heal wounds, Biomaterials 27 (2006) 145–151.
[19] X. Wang, F. Cheng, J. Liu, J.-H. Smått, D. Gepperth, M. Lastusaari, C. Xu, L. Hupa, Biocomposites of copper-containing mesoporous bioactive glass and nanofibrillated cellulose: biocompatibility and angiogenic promotion in chronic wound healing application, Acta Biomater. 46 (2016) 286–298.
[20] S. Homaeigohar, A.R. Boccaccini, Antibacterial biohybrid nanofibers for wound dressings, Acta Biomater. 107 (2020) 25–49.
[21] N. Li, L. Yang, C. Pan, P.E. Saw, M. Ren, B. Lan, J. Wu, X. Wang, T. Zeng, L. Zhou, L.-M. Zhang, C. Yang, L. Yan, Naturally-occurring bacterial cellulose-hyperbranched cationic polysaccharide derivative/MMP-9 siRNA composite dressing for wound healing enhancement in diabetic rats, Acta Biomater. 102 (2020) 298–314.
[22] K. Bethke, S. Palantöken, V. Andrei, M. Roß, V.S. Raghuwanshi, F. Kettemann, K. Greis, T.T.K. Ingber, J.B. Stückrath, S. Valiyaveettil, Functionalized cellulose for water purification, antimicrobial applications, and sensors, Adv. Funct. Mater. 28 (2018) 1800409.
[23] R. Weishaupt, J.N. Zünd, L. Heuberger, F. Zuber, G. Faccio, F. Robotti, A. Ferrari, G. Fortunato, Q. Ren, K. Maniura-Weber, Antibacterial, cytocompatible, sustainably sourced: cellulose membranes with bifunctional peptides for advanced wound dressings, Adv. Healthc. Mater. 9 (2020) 1901850.
[24] S. Roig-Sanchez, E. Jungstedt, I. Anton-Sales, D.C. Malaspina, J. Faraudo, L.A. Berglund, A. Laromaine, A. Roig, Nanocellulose films with multiple functional nanoparticles in confined spatial distribution, Nanoscale Horizons 4 (2019) 634–641.
[25] I. Anton-Sales, S. Roig-Sanchez, M.J. Sánchez-Guisado, A. Laromaine, A. Roig, Bacterial Nanocellulose and Titania Hybrids: Cytocompatible and Cryopreservable Cell Carriers, ACS Biomater. Sci. Eng. 6 (2020) 4893–4902.
[26] T. Maneerung, S. Tokura, R. Rujiravanit, Impregnation of silver nanoparticles into bacterial cellulose for antimicrobial wound dressing, Carbohydr. Polym. 72 (2008) 43–51.
[27] I.S. Savitskaya, D.H. Shokatayeva, A.S. Kistaubayeva, L.V. Ignatova, I.E. Digel, Antimicrobial and wound healing properties of a bacterial cellulose based material containing B, Subtilis Cells, Heliyon 5 (2019) e02592.
[28] M. Schramm, S. Hestrin, Factors affecting production of cellulose at the air/liquid interface of a culture of Acetobacter xylinum, J. Gen. Microbiol. 11 (1954) 123–129.
[29] L. Herman, M. Chemaly, P.S. Cocconcelli, P. Fernandez, G. Klein, L. Peixe, M. Prieto, A. Querol, J.E. Suarez, I. Sundh, J. Vlak, S. Correia, The qualified presumption of safety assessment and its role in EFSA risk evaluations: 15 years past, FEMS Microbiol. Lett. 366 (2019) 1–7.
[30] G. Serafica, R. Mormino, G.A. Oster, K.E. Lentz, K.P. Koehler, Microbial cellulose wound dressing for treating chronic wounds, U.S. Patent No. 7,704,523., 2010.
[31] S.C. Becerra, D.C. Roy, C.J. Sanchez, R.J. Christy, D.M. Burmeister, An optimized staining technique for the detection of gram positive and gram negative bacteria within tissue, BMC Res. Notes. 9 (2016) 1–10.
[32] Y. Hu, J.M. Catchmark, Integration of cellulases into bacterial cellulose: toward bioabsorbable cellulose composites, J. Biomed. Mater. Res. Part B Appl. Biomater. 97 (2011) 114–123.
[33] K. Chi, J.M. Catchmark, The influences of added polysaccharides on the properties of bacterial crystalline nanocellulose, Nanoscale 9 (2017) 15144–15158.
[34] A. González, N. Gálvez, M. Clemente-León, J.M. Dominguez-Vera, Electrochromic polyoxometalate material as a sensor of bacterial activity, Chem. Commun. 51 (2015) 10119–10122.
[35] S. Tejero-Sariñena, J. Barlow, A. Costabile, G.R. Gibson, I. Rowland, In vitro evaluation of the antimicrobial activity of a range of probiotics against pathogens: evidence for the effects of organic acids, Anaerobe 18 (2012) 530–538.
[36] A. Khalid, R. Khan, M. Ul-Islam, T. Khan, F. Wahid, Bacterial cellulose-zinc oxide nanocomposites as a novel dressing system for burn wounds, Carbohydr. Polym. 164 (2017) 214–221.
[37] M. Balouiri, M. Sadiki, S.K. Ibnsouda, Methods for in vitro evaluating antimicrobial activity: a review, J. Pharm. Anal. 6 (2016) 71–79.
[38] Y. Wang, V. Leng, V. Patel, K.S. Phillips, Injections through skin colonized with Staphylococcus aureus biofilm introduce contamination despite standard antimicrobial preparation procedures, Sci. Rep. 7 (2017) 45070.
[39] Y. Wang, X. Tan, C. Xi, K.S. Phillips, Removal of Staphylococcus aureus from skin using a combination antibiofilm approach, NPJ Biofilms Microbiomes 4 (2018) 1–9.
[40] M. Olivares, M.P. Díaz-Ropero, R. Martín, J.M. Rodríguez, J. Xaus, Antimicrobial potential of four Lactobacillus strains isolated from breast milk, J. Appl. Microbiol. 101 (2006) 72–79.
[41] R. Martín, S. Langa, C. Reviriego, E. Jimínez, M.L. Marín, J. Xaus, L. Fernández, J.M. Rodríguez, Human milk is a source of lactic acid bacteria for the infant gut, J. Pediatr. 143 (2003) 754–758.
[42] K. Gjødsbøl, J.J. Christensen, T. Karlsmark, B. Jørgensen, B.M. Klein, K.A. Krogfelt, Multiple bacterial species reside in chronic wounds: a longitudinal study, Int. Wound J. 3 (2006) 225–231.
[43] A. González, L. Sabio, C. Hurtado, G.B. Ramírez-Rodríguez, V. Bansal, J.M. Delgado-López, J.M. Dominguez-Vera, Entrapping living probiotics into collagen scaffolds: a new class of biomaterials for antibiotic-free therapy of bacterial vaginosis, Adv. Mater. Technol. 5 (2020) 2000137.
[44] Z. Li, A.M. Behrens, N. Ginat, S.Y. Tzeng, X. Lu, S. Sivan, R. Langer, A. Jaklenec, Biofilm-inspired encapsulation of probiotics for the treatment of complex infections, Adv. Mater. 30 (2018) 1803925.
[45] J. Kwiecinski, G. Kahlmeter, T. Jin, Biofilm formation by staphylococcus aureus isolates from skin and soft tissue infections, Curr. Microbiol. 70 (2015) 698–703.
[46] A.V. Oliveira-Alcântara, A.A.S. Abreu, C. Gonçalves, P. Fuciños, M.A. Cerqueira, F.M.P. da Gama, L.M. Pastrana, S. Rodrigues, H.M.C. Azeredo, Bacterial cellulose/cashew gum films as probiotic carriers, LWT (2020) 109699.
[47] R.T. Olsson, M.A.S. Azizi Samir, G. Salazar-Alvarez, L. Belova, V. Ström, L.A. Berglund, O. Ikkala, J. Nogués, U.W. Gedde, Making flexible magnetic aerogels and stiff magnetic nanopaper using cellulose nanofibrils as templates, Nat. Nanotechnol. 5 (2010) 584–588.
[48] M. Gao, J. Li, Z. Bao, M. Hu, R. Nian, D. Feng, D. An, X. Li, M. Xian, H. Zhang, A natural in situ fabrication method of functional bacterial cellulose using a microorganism, Nat. Commun. 10 (2019) 437.